

mass of the disperse material, kg;  $G_T$ , mass flow rate of disperse material, kg/s;  $S$ , cross section of the channel,  $m^2$ ;  $G_S = G_T/S$ , specific load of disperse material,  $kg/(m^2 \cdot sec)$ ;  $p$ , pressure,  $N/m^2$ ;  $g$ , acceleration due to gravity,  $m/sec^2$ ;  $\beta = G_S/w$ , dustiness of the gas,  $kg/m^3$ ;  $\rho_S$ , saturation density of the bed of disperse material,  $kg/m^3$ ;  $\rho$ , density of the fluidized bed,  $kg/m^3$ ;  $\tau$ , dwell time of the disperse material in the bed, sec. Subscripts:  $i, j$ , number of points; bar above - mean value.

#### LITERATURE CITED

1. I. M. Razumov, Pneumatic and Hydro-Transport in the Chemical Industry [in Russian], Moscow (1979).
2. J. Yerushalmi, D. H. Turner, and M. Squires, Ind. Eng. Chem., Processes Des. Dev., Vol. 15, No. 1, 47-53 (1976).

#### EXTERNAL HEAT TRANSFER IN AN ELECTRODYNAMICALLY FLUIDIZED BED

M. K. Bologa, A. B. Berkov,  
and V. L. Solomyanchuk

UDC 541.182.3:537.212

Heat-transfer trends are considered for a granular bed fluidized by electrical forces in a controlled gas atmosphere or under high vacuum.

A granular material can be fluidized by various means: hydrodynamically with a gas or liquid or by vibration, etc., which can greatly accelerate heat and mass transfer at immersed surfaces and between components [1-4]; it is widely used in engineering. Particle electrification during fluidization is usually considered an adverse effect that tends to reduce the heat transfer [2] because of aggregation and reduced mobility, with the heat-transfer surfaces being obstructed by electrically bound particles. It is found [5, 6] that strong external electric fields are ineffective in influencing the hydromechanics and heat transfer in pneumatically fluidized insulating-granule beds. However, if the particles are conducting or semiconducting, they can be agitated vigorously by Coulomb forces [7], i.e., one can provide an electrodynamically fluidized bed. Some trends in such fluidization [7, 8] indicate that it is promising for use with low energy input and fine control. The trends in heat transfer for a planar horizontal electrodynamically fluidized bed [8-10] indicate that the transfer can be accelerated by up to a factor 80 by comparison with a gas layer, and this also provides some evidence on the heat-transfer mechanism there.

We have examined the heat transfer in such a bed for fairly wide ranges in the particle and dispersion-medium characteristics in order to identify the mechanism and extend the measurements.

We used stationary transfer conditions for a homogeneous part of a planar bed (Fig. 1), which was located in a sealed chamber on a vacuum line; this enabled us to examine the transfer under high vacuum or in a medium isolated from the atmosphere having the required composition and pressure. The fluidization was produced in a horizontal model having height  $h = 10$  mm (Fig. 1) with upper heat-supply and lower cooled electrodes separated by a transparent ring insulator (lucite). At the edge of the gap adjoining the insulator, there were convergent conical parts representing electrostatic seals, angle between them  $5.4^\circ$ , while the outer boundary was a circle 200 mm in diameter. Those seals localized the fluidization in the inner plane-parallel part and ensured electrical strength for the inner insulator surface.

The stationary state was established, with the heat losses balanced by an isothermal jacket (Fig. 1), where we determined the heat-transfer coefficient  $K$  through the fluidized

---

Applied Physics Institute, Moldavian Academy of Sciences, Kishinev. Translated from Inzhenerno-Fizicheskii Zhurnal, Vol. 57, No. 5, pp. 767-774, November, 1989. Original article submitted May 11, 1988.

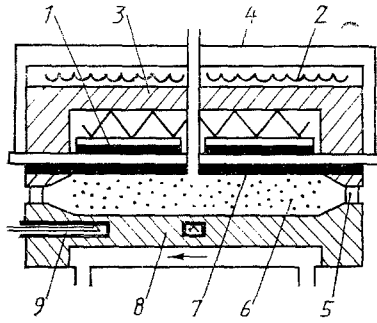


Fig. 1

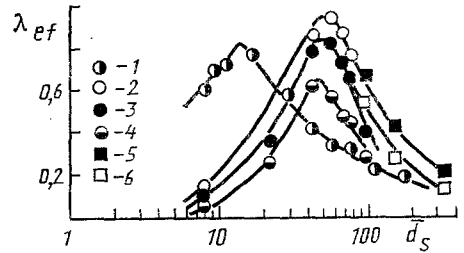


Fig. 2

Fig. 1. The model: 1) main heater (resistance thermometer); 2) guard heater; 3) isothermal shell (high conductivity); 4) thermal insulation; 5) transparent insulating ring; 6) electro-dynamically fluidized bed; 7) heat-supply (grounded) electrode; 8) cooled (high-voltage) electrode; 9) thermocouples.

Fig. 2. Dependence of the effective thermal conductivity for fluidized bed  $\lambda_{ef}$  in W/m·K on mean particle diameter  $d_s$  in  $\mu\text{m}$ : 1) bronze; 2-4) stainless steel; 5 and 6) psilomelane, all fluidies in gases at atmospheric pressure: 1, 2, 5, and 6) in air; 3) carbon dioxide; 4) in freon-12 vapor; 1-4)  $\beta = 7.76 \cdot 10^{-3}$ ,  $E = 7$  kV/cm, our results; 5 and 6)  $\beta = 2 \cdot 10^{-2}$ ,  $E = 9$ ; 6 kV/cm, [8] data.

region and the effective thermal conductivity  $\lambda_{ef}$ :

$$K = \frac{Q_b}{F(t_h - t_c)}; \quad \lambda_{ef} = Kh. \quad (1)$$

We used stainless-steel particles with mean diameters  $\bar{d}_s$  for the fractions in the range 8-95  $\mu\text{m}$ , bronze with 8-180  $\mu\text{m}$ , and copper and graphite with 42.4  $\mu\text{m}$ , mean volume concentrations  $\beta = 0.05$ -1%. The gases were air at from  $2 \times 10^{-3}$  to  $10^5$  Pa, carbon dioxide, and freon-12 vapor at atmospheric pressure. The mean field strength in the gas varied from the threshold (fluidization onset)  $E_i = 3$  kV/cm to the breakdown  $E_{br} = 10$ -13 kV/cm.

The heat transfer was examined when the electrical strength in the gas adequate, which corresponded to pressures  $p \gtrsim 2 \cdot 10^4$  Pa and  $p \lesssim 1$  Pa. The transfer in the first range was more rapid by 1-2 orders of magnitude than in the second. The pressure dependence of  $\lambda_{ef}$  corresponds to the [11] data on transfer in vibrationally fluidized beds as the air pressure is reduced from atmospheric.

The effects of the mean field strength on the effective transfer characteristics in the first range ( $p \gtrsim 2 \cdot 10^4$  Pa) correspond to data from other sources for electrodynamic fluidization in air [9] and liquids [12, 13]; the relationship is  $\lambda_{ef} \sim \bar{E}^n$ , with  $0 < n < 1$ , while the monotone rise in  $\lambda_{ef}$  with  $\bar{E}$  in the second range (high vacuum) is much less pronounced, being only a few tens of percent throughout the fluidization range. The  $\bar{E}$  dependence of  $\lambda_{ef}$  as a measure of the fluidization here is essentially different from the results for hydrodynamic case, an increase in  $\bar{E}$  raises the particle speed, which is not accompanied by a reduction on  $\beta$ , and there is a monotone increase in  $\lambda_{ef}$ .

The  $\beta$  dependence of  $\lambda_{ef}$  corresponds to published data [8, 9, 12, 13], as  $\lambda_{ef}$  increases to a maximum and then stabilizes or falls. The  $\beta$  corresponding to the maximum is the critical value  $\beta_{cr}$  and corresponds to the onset of particle deposits forming on the lower electrode [14, 15].

There is a fairly marked dependence of  $\lambda_{ef}$  on the conductivity of the fluidizing medium  $\lambda_f$ . For electrically neutral suspended beds, this is usually approximated as ( $\lambda_{ef} \sim \lambda_f^n$ , with  $n = 0.6$ -0.7 [2]), or else in exponential form [1]. Our results can be fitted to  $\lambda_{ef} = 7.85\lambda_f + B$ , in which B is a constant coefficient characterizing transfer through the bed for the parameters used.

The temperature difference has only a slight effect on  $\lambda_{ef}$ , as in the [8, 12] experiments, in the fluidization of bronze and graphite particles in a gas at pressures close to atmospheric. In those cases, the rate of increase in  $\lambda_{ef}$  with the mean temperature in the bed ( $5 \times 10^{-4} \text{ W/m}\cdot\text{K}^2$ ) exceeds the temperature coefficient for the thermal conductivity of air ( $7.7 \times 10^{-5} \text{ W/m}\cdot\text{K}^2$ ). Stainless-steel particles showed a more marked increase in  $\lambda_{ef}$  with mean temperature ( $6.7 \times 10^{-3} \text{ W/m}\cdot\text{K}^2$ ), which is due to the temperature influencing the dispersant motion (this is seen as structuring, which was identified for this powder by varying the specific charging level, and by other effects).

Figure 2 shows how  $\lambda_{ef}$  varies with the particle size for narrow fractions  $\lambda_{ef}(\bar{d}_s)$  has a maximum in a gas near atmospheric pressure, which has not been identified previously [8-10, 12]. The optimum size as regards transfer and separation (some tens of microns) corresponds to the size providing the maximum mean velocity and heat transport [15, 16]. The peak in  $\lambda_{ef}(\bar{d}_s)$  corresponds qualitatively to the variation in external heat transfer rate with size in hydrodynamically and vibrationally fluidized beds [17]. The minimum in the transfer occurring for electrically neutral beds is not found with electrodynamic fluidization, since here the fairly large particles for which one expects the minimum (about 1 mm) require mean field strengths substantially exceeding the breakdown values for the gases used. Under high vacuum,  $\lambda_{ef}(\bar{d}_s)$  for bronze has a fairly flat maximum, while stainless steel gives a monotonically decreasing curve.

A limit to the amount of electrically suspended material in this fluidization is set by  $\beta_{cr}$  [14] at mean distances between particles greatly exceeding the size, so in electrodynamic fluidization, as in a low-concentration flow system (gas suspensate), one can get a thermal boundary layer separating the transfer surface from the almost isothermal bed core. The heat is transferred from the electrode to the core in an electrodynamically fluidized bed in two ways: by conduction through the thermal boundary layer and by particles heated in that layer that transport the heat to the core. In a concentrated electrically neutral fluidized bed, the first mechanism is lacking because the boundary layer is disrupted by the continuous bombardment by the dense particle layer [1].

The thickness  $\delta_t$  of the thermal boundary layer is governed by the hydrodynamic boundary layer thickness  $\delta_g$  and the Prandtl number for the dispersion medium  $Pr$ , so the thermal resistance there is

$$\frac{1}{\alpha_{E,1}} = \frac{\delta_t}{\lambda_f} = \frac{\delta_g Pr^{-m}}{\lambda_f} = \frac{0.807 A_1 \bar{d}_s Pr^{-m}}{A_0^{n_1} \lambda_f Re_{s,0}^{n_1} \bar{\beta}^{(1/3-n_0 n_1)}}, \quad (2)$$

which reflects the proportionality between  $\delta_g$  and the mean particle separation ( $0.807 \bar{d}_s / \bar{\beta}^{1/3}$ ), as well as the reduction in  $\delta_g$  as the Reynolds number for the particles colliding with the electrodes increases ( $\delta_g \sim Re_s^{-n_1}$ ) (2) incorporates

$$Re_s = A_0 Re_{s,0} \bar{\beta}^{n_0}; \quad 0 < n_0 < 1, \quad (3)$$

which describes the reduction in particle speed near the electrodes as  $\bar{\beta}$  increases. We introduce the Nusselt number  $Nu_{E,1}$  to convert (2) to dimensionless form

$$Nu_{E,1} = A_2 Re_{s,0}^{n_1} Pr^m \bar{\beta}^{(1/3-n_0 n_1)}, \quad (4)$$

in which  $A_2 = A_0^{n_1} / 0.807 A_1$ .

The second mechanism appears [13] to be uniquely responsible for the substantial acceleration in heat transfer under these conditions. To estimate its contribution, we represent the fluidized bed as a two-layer structure: two thermal boundary layers at the electrode surfaces and an almost isothermal core, temperature  $t_\psi$ . When a particle contacts an electrode, heat is transferred through the gas lens, and the heat flux density  $q_2$  is governed by the flux density for the dispersing agent at the electrode [16] carried by the isothermal particles having  $Bi_s < 0.1$  (which exchange heat with the dispersion medium in the boundary layer in time  $\tau$ ):

$$q_2 = \frac{\rho_s c_s}{2} \frac{\bar{\beta} h}{T} (t_w - t_\psi) \{1 - \exp[-6\alpha_s \tau / (\rho_s c_s \bar{d}_s)]\}. \quad (5)$$

We transform this to dimensionless form and combine it with (4) to get a general expression for the heat transfer to the bed from the electrode:

$$Nu_{E,\alpha} = A_2 Re_{s,0}^{n_1} Pr^m \bar{\beta}^{(1/3-n_0 n_1)} + A_4 \frac{\rho_s c_s}{\rho_f c_f} Pe_{s,0} \bar{\beta}^{(1-n_0)} [1 - \exp(-1.5 Bi_s Fo_s)], \quad (6)$$

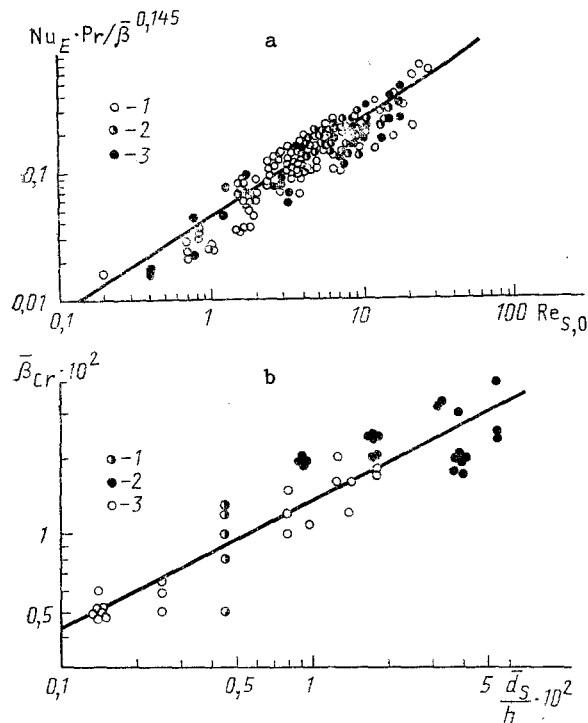


Fig. 3. Data on heat transfer (a) and critical mean volume dispersant concentration (b) for electrodynamic fluidization for narrow fractions of aluminum, bronze, graphite, titanium, copper, copper oxide, stainless steel, nickel, psilomelane, and pyrolucite for bed parameters in the ranges  $\bar{d}_s = 5.5$ – $354 \mu\text{m}$ ,  $\bar{\beta} = 5 \cdot 10^{-4}$ – $3.5 \cdot 10^{-3}$ ,  $\bar{E} = 2$ – $18 \text{ kV/cm}$ : 1) our results; 2) [8]; 3) [9].

in which  $Pe_{S,0} = Re_{S,0} Pr_{\bar{\beta}}$  is the Peclet number for the dispersion agent calculated from the mean velocity for small  $\bar{\beta}$ ,  $Fo_S$  is the Fourier number for the particles calculated from the mean time spent in the boundary layer, and  $A_4 = 0.25A_0$ . The external heat-transfer rate is then independent of the gas pressure at  $p \approx 2 \cdot 10^4 \text{ Pa}$  because the thermal conductivity and viscosity are only slightly dependent on pressure. Our experiments and those described in [9, 10] confirm that the heat-transfer characteristics here are independent of air pressure in the range  $2 \cdot 10^4 < p \leq 6 \cdot 10^5 \text{ Pa}$ .

One can simplify (6) in two limiting cases. If one has thermally slow (fairly large) particles in a low-conductivity medium (gas), then  $1.5Bi_S Fo_S \ll 1$ , in which case the particles become only slightly heated or cooled on interacting with the electrode boundary layers, and (6) on the basis of correlations [18, 19] for heat transfer between components in an unconstrained gas suspension becomes

$$Nu_{E,\alpha} = A_2 Re_{S,0}^{n_1} Pr^{m_1} \bar{\beta}^{(1/3-n_0 n_1)} + A_5 Re_{S,0}^{(0.79-n_1)} \bar{\beta}^{(2/3-1.79 n_0)} Pr^{-m_1}, \quad (7)$$

in which  $A_5 = 0.235 A_0^{1.79} A_1 A_6 (1 + |k_n|^{-1})$ ;  $A_6 = \bar{V}_{s,0} / V_{s,e}$ . (7) gives the form in which the data may be fitted for external heat transfer in such a system.

In [8], the data on heat transfer in such a fluidized bed in air ( $Pr = 0.696$ ) were fitted with  $\pm 20\%$  error to

$$Nu_{E,K} = 0.784 (0.5 Re_{S,0} \bar{\beta})^{0.31}, \quad (8)$$

which is applicable for  $4 \leq Re_{S,0} < 16$ ;  $0.00125 \leq \bar{\beta} \leq 0.025$ . The model there does not incorporate heat transport by the particles, although (8) corresponds in form to (4) if one bears in mind that  $Pr^m = \text{const} \approx 1$  for air and one assumes that the exponents are equal at 0.31 for  $Re_{S,0}$  and  $\bar{\beta}$  in (4) ( $n_1 = 1/3 - n_0 n_1 \approx 0.31$ ). It was assumed in [8] that the main contribution to the heat transfer through the bed comes from the gas adhering to the particles, which requires refinement, since the bulk specific heat of the gas is substantially less than that of the particles ( $\rho_f c_f \ll \rho_s c_s$ ), while the concentrations are approximately equal.

We processed our data and those from [8-10] from (7) as a relation between  $Nu_{E,K}$  and  $Re_{s,0}$ ,  $\beta$  and Pr together with Pr for the following ranges:  $0.2 \leq Re_{s,0} \leq 30$ ;  $0 < \beta < \beta_{cr}$   $\leq 0.035$ ;  $0.69 \leq Pr \leq 0.98$  (Fig. 3a). The results can be represented with an error of  $\pm 50\%$  as

$$Nu_{E,K} = 0,044 Re_{s,0}^{0,752} Pr^{-1} \bar{\beta}^{0,145}. \quad (9)$$

The fitting was for the range  $\bar{\beta} \leq \bar{\beta}_{cr}$ , with  $\bar{\beta}_{cr}$  defined [15] by  $\bar{d}_s/h$ . The formula

$$\bar{\beta}_{cr} = 0,13 (\bar{d}_s/h)^{0,5} \quad (10)$$

fits the [8-10] data and ours for  $1.4 \cdot 10^{-3} \leq \bar{d}_s/h \leq 5.4 \cdot 10^{-2}$  (Fig. 3b).

In the second limit  $1.5 Bi_s Fo_s \gg 1$ , which applies for fast-responding (small) particles fluidized in an insulating medium with high thermal conductivity (liquid), (6) simplifies to

$$Nu_{E,\alpha} = A_2 Re_{s,0}^{n_1} Pr^m \bar{\beta}^{(1/3-n_0n_1)} + A_4 \frac{\rho_s c_s}{\rho_f c_f} Pe_{s,0} \bar{\beta}^{(1-n_0)}. \quad (11)$$

Similar equations have been proposed [12] for heat transfer from a disk to an insulating-liquid emulsion or a suspension of conducting particles, which for suspensions was

$$Nu_{E,D} = 0,46 \{(\varepsilon \bar{E}^2 D^2 Pr) / (\rho_f v_f^2)\}^{0,36} \bar{\beta}^{0,33} (Pr_f / Pr_w)^{0,25}. \quad (12)$$

When the similarity numbers have been transformed to the (11) form, we get

$$Nu_{E,\alpha} = 0,08 Pe_{s,0}^{0,36} \bar{\beta}^{0,33}, \quad (13)$$

in which we have used the fact that  $0.46(18/\pi^2)^{0,36} (\bar{d}_s/D)^{0,28} (Pr_w)^{0,25}$  is about 0.08 for the orders of the quantities used in the experiments,  $O(\bar{d}_s) = 10 \mu m$  and  $O(D) = 10^{-2}$  and for small temperature differences  $(Pr_f / Pr_w)^{0,25} \approx 1$  and for small temperature differences. Equation (13) describes the external heat transfer to an electrodynamically fluidized suspension of electrically conducting particles in an insulating liquid for  $\beta < \beta_{cr}$ .

The substantial acceleration in heat transfer through an electrodynamically fluidized bed means that it can be used in a gas-suspension heat exchanger to provide widely controlled thermal resistance, as used in devices designed to provide a given heat uptake from surfaces and appropriate heat-treatment conditions for workpieces. Equations (9) and (13) also enable one to design thermostatic devices viable in the presence of variable mass forces and under micro-gravity conditions.

#### NOTATION

$A_0$ - $A_6$ , positive dimensionless constants in equations;  $a$ , thermal diffusivity;  $Bi_s = \alpha_s \bar{d}_s / \lambda_s$ , particle Biot number;  $c$ , specific heat;  $d$ , heat-output disk diameter;  $\bar{d}_s$ , mean particle diameter;  $\bar{E}$ , mean field strength between electrodes;  $F$ , heat-transfer area;  $Fo_s = 4a_s \tau / \bar{d}_s^2$ , particle Fourier number;  $h$ , electrode gap;  $k_n$ , recovery coefficient for normal velocity component of particle on collision with electrode;  $Nu_{E,\alpha} = \alpha_E \bar{d}_s / \lambda_f$ ;  $Nu_{E,K} = K \bar{d}_s / \lambda_f$ ;  $Nu_{E,i} = \alpha_{E,i} \bar{d}_s / \lambda_f$ ;  $Nu_{E,D} = \alpha_E D / \lambda_f$ , Nusselt numbers describing external heat transfer and heat transmission in electrodynamically fluidized bed;  $n_0$ ,  $n_1$ , and  $m$ , positive dimensionless exponents in equations;  $Pe_{s,0} = \bar{V}_{s,0} \bar{d}_s / a_f$ , Peclet number for dispersant;  $Pr = v_f / a_f$ , Prandtl number;  $Pr_f$  and  $Pr_w$ , Prandtl numbers for fluidizing medium reckoned from defining temperature of medium and wall correspondingly;  $p$ /gas pressure;  $Q$ , heater power;  $Re_s = \bar{V}_s \bar{d}_s / v_f$ ;  $Re_{s,0} = \bar{V}_{s,0} \bar{d}_s / v_f$ , Reynolds numbers for particle;  $T$ , mean particle motion period in fluidized bed;  $t$ , temperature;  $V_s$ ,  $\bar{V}_{s,0}$ , and  $V_{s,e}$ , local velocity, mean velocity between electrodes for small mean volume particle concentrations, and velocity of particles colliding with electrode;  $\alpha_E$  and  $\alpha_{E,1}$ , total heat-transfer coefficient for electrode surface and heat-transfer coefficient due to electrode boundary layer;  $\beta$ , mean volume particle concentration;  $\delta$ , boundary layer thickness;  $\varepsilon$ , dispersion-medium dielectric constant;  $\lambda$ , thermal conductivity;  $v_f$ , kinematic viscosity of dispersion medium;  $\rho$ , density;  $\tau$ , mean particle residence time in electrode thermal boundary layer. Subscripts;  $b$ , basic heater;  $br$ , electrical breakdown;  $c$ , heat-collecting electrode;  $cr$ , critical;  $E$ , value of quantity in electrodynamically fluidized bed;  $ef$ , effective value;  $f$ , fluidizing medium;  $g$ , hydrodynamic boundary layer;  $h$ , heat-output electrode;  $i$ , start of electrodynamic fluidization;  $0$ , low mean volume fluidizing agent concentration;  $s$ , dispersant;  $t$ , thermal boundary layer.

## LITERATURE CITED

1. S. S. Zabrodskii, *Hydromechanics and Heat Transfer in Fluidized Beds* [in Russian], Moscow-Leningrad (1963).
2. *Fluidization* [in Russian], Moscow (1974).
3. J. Botterill, *Heat Transfer in Fluidized Beds* [Russian translation], Moscow (1980).
4. V. A. Chlenov and N. V. Mikhailov, *Vibrationally Fluidized Beds* [in Russian], Moscow (1972).
5. W. J. Thomas and R. J. Melcher, *Ind. Eng. Chem. Fundamentals*, 14, No. 3, 140-153 (1975).
6. R. Eldson and C. J. Shearer, *Chem. Eng. Sci.*, 32, No. 10, 1147-1153 (1977).
7. O. A. Myazdrikov, *Electrodynamic Fluidization in Dispersed Systems* [in Russian], Leningrad (1984).
8. V. V. Pushkov, Z. R. Gorbis, and M. K. Bologa, *Inzh.-Fiz. Zh.*, 27, No. 2, 253-259 (1974).
9. Yu. E. Tetelya, V. V. Vishnevskii, V. P. Usenko, et al., *EOM*, No. 4, 61-64 (1984).
10. M. K. Bologa, V. V. Pushkov, and Yu. E. Tetelya, *Proceedings of the 3rd All-Union Conference on Electron-Ion Technology Applications* [in Russian], Tbilisi (1981), p. 16.
11. B. G. Sapozhnikov and N. I. Syromyatnikov, *Izv. Vyssh. Uchebn. Zaved., Energ.* No. 5, 116-119 (1969).
12. M. K. Bologa, F. P. Grosu, and I. A. Kozhukhar', *Electroconvection and Heat Transfer* [in Russian], Kishinev (1977).
13. P. W. Dietz and J. R. Melcher, *Trans. ASME*, C97, No. 3, 429-434 (1975).
14. M. K. Bologa and A. B. Berkov, *Inzh.-Fiz. Zh.*, 53, No. 1, 77-84 (1977).
15. A. B. Berkov, *Accelerating Heat Transfer and the Motion of Electrically Conducting Particles in a Gas-Fluidized System in the Presence of an Electric Field: Ph. D. Thesis* [in Russian], Kishinev (1985).
16. M. K. Bologa, V. V. Pushkov, and A. B. Berkov, *Izv. Akad. Nauk SSSR, Energ. Transport*, No. 4, 109-116 (1980).
17. S. S. Zabrodskii, I. L. Zamnius, S. A. Malyukovich, et al., *Inzh.-Fiz. Zh.*, 14, No. 3, 448-453 (1968).
18. M. K. Bologa, V. V. Pushkov, and A. B. Berkov, *Int. J. Heat Mass Transfer*, 28, No. 7, 1245-1255 (1985).
19. Z. R. Gorbis, *Heat Transfer and Hydromechanics for Dispersed Through Flows* [in Russian], Moscow (1970).

FLUID DISTRIBUTION IN THE GRANULAR LAYER FOR A  
DESCENDING GAS-LIQUID STREAM

V. M. Khanaev, V. A. Kirillov,  
V. A. Kuz'min, and Yu. A. Malkov

UDC 532.529.5:532.546

The flow of a fluid in an irrigatable granular layer is investigated experimentally.

In catalytic reactors with a fixed granular layer in which a descending gas-liquid stream is used, the liquid distribution over the layer is of great value. The appearance of stream inhomogeneities results in a reduction in reactor productivity and causes additional difficulties in the control and regulation of the process [1] as well as in its mathematical description.

At this time there is not a well-founded quantitative description of the gas-liquid stream flow inhomogeneities in a layer because of the inadequacy of experimental data. Annular coaxial liquid collectors mounted at the exit from the layer that are used to determine the velocity profile along the radius of the apparatus [2-4] are ordinarily utilized in experimental investigations. But as is shown in [5], significant local stream inhomogenei-

---

Catalysis Institute, Siberian Branch, Academy of Sciences of the USSR, Novosibirsk.  
Translated from *Inzhenerno-Fizicheskii Zhurnal*, Vol. 57, No. 5, pp. 774-779, November, 1989.  
Original article submitted March 23, 1988.